

#### **OPEN ACCESS**

EDITED BY Shude He, Guangzhou University, China

REVIEWED BY
Mario Versaci,
Mediterranea University of Reggio Calabria,
Italy
Isak Karabegović,
University of Bihać, Bosnia and Herzegovina

\*CORRESPONDENCE
Sha Luo

I luosha320@126.com
Qingdang Li
I lqd@qust.edu.cn

†These authors share first authorship

RECEIVED 10 February 2025 ACCEPTED 25 August 2025 PUBLISHED 13 November 2025

#### CITATION

Zhuang Y, Luo S, Li Q, Chu D, Bai W, Liu X, Fan M and Wei L (2025) Path planning of industrial robots based on the adaptive field cooperative sampling algorithm. *Front. Neurorobot.* 19:1574044. doi: 10.3389/fnbot.2025.1574044

### COPYRIGHT

© 2025 Zhuang, Luo, Li, Chu, Bai, Liu, Fan and Wei. This is an open-access article distributed under the terms of the Creative Commons Attribution License (CC BY). The use, distribution or reproduction in other forums is permitted, provided the original author(s) and the copyright owner(s) are credited and that the original publication in this journal is cited, in accordance with accepted academic practice. No use, distribution or reproduction is permitted which does not comply with these terms.

# Path planning of industrial robots based on the adaptive field cooperative sampling algorithm

Yongbo Zhuang<sup>1†</sup>, Sha Luo<sup>1\*†</sup>, Qingdang Li<sup>1\*</sup>, Dianming Chu<sup>1</sup>, Wenjuan Bai<sup>1</sup>, Xintao Liu<sup>1</sup>, Mingyuan Fan<sup>1</sup> and Lv Wei<sup>2</sup>

<sup>1</sup>College of Electromechanical Engineering, Qingdao University of Science and Technology, Shandong Province, China, <sup>2</sup>Shandong Gaomi Technician Institute, Shandong Province, China

For the low efficiency and poor generalization ability of path planning algorithm of industrial robots, this work proposes an adaptive field co-sampling algorithm (AFCS). Firstly, the environment complexity function is proposed to make full use of environment information and improve its generalization ability of the traditional rapidly random search tree algorithm (RRT) algorithm. Then an optimal sampling strategy is proposed to make the improvement of the efficiency and optimal direction of RRT algorithm. Finally, this article designs a collaborative extension strategy, which introduces the improved artificial potential field algorithm (APF) into the traditional RRT algorithm to determine the new nodes, so as to improve the orientation and expansion efficiency of the algorithm. The proposed AFCS algorithm completes simulation experiments in two environments with different complexity. Compared with the traditional RRT, RRT\* and tRRT algorithm, the results show that the AFCS algorithm has achieved great improvement in environmental adaptability, stability and efficiency. At last, ROKAE industrial robot is taken as the object to build a simulation environment for the path planning, which further verifies the practicability of the algorithm.

KEYWORDS

industrial robot, path planning, RRT, APF, AFCs

### 1 Introduction

Recently, the demand for intelligent robots is gradually increasing with the continuous development of artificial intelligence technology. Especially for industrial robots, path planning is a decisive factor to determine their safe operation. It refers to the autonomous planning of industrial robots in their configuration space to find a continuous non-collision smooth path between the initial pose and the target pose in order to reach the preset target pose when moving in the surrounding static and dynamic obstacle environment. Meanwhile, it must meet various constraints such as environmental, time and dynamic constraints of industrial robots (Wei and Ren, 2018). Different from that of mobile robots, it is more complex for industrial robots to realize path panning. It not only needs to consider constraints such as obstacles, but also involves the mutual transformation of joint space and configuration space. Therefore, the path planning algorithm of mobile robots is not completely applicable to the path planning of industrial robots. At present, there are three kinds of path planning algorithms of industrial robots: traditional obstacle avoidance planning method (Khatib, 1986; Hart et al., 1972), intelligent obstacle avoidance planning algorithm (Guan-Zheng and Huan, 2007; Kavraki et al., 1994), sampling-based obstacle avoidance planning algorithm (Lavalle, 1998; Karman and Frazzoli, 2011). Among them, the sample-based RRT algorithm (Lavalle, 1998) is the most applicable one in path planning algorithms of industrial robots, who has the characteristics of probability completeness and high dimensional space applicability (Lixing

Liu et al., 2023). And it was also proved that the sample-based RRT algorithm owned the better efficiency and more smoother path than the intelligent obstacle avoidance planning algorithm for the industrial robots (Larsena, 2017). However, the traditional RRT algorithm has some problems such as redundant sampling, low efficiency and non-optimal path, which limit its generalization ability in complex environment (Jia et al., 2022). For these problems, research and improvement of RRT algorithm is a hot topic pursued by many scholars.

Among the variants of RRT algorithm, neither RRT algorithm, RRT\* algorithm (Karman and Frazzoli, 2011) nor Informed RRT\* algorithm (Gammell et al., 2014) fundamentally solve the randomness, low efficiency and optimality. Especially, in the sampling stage, redundant sampling brings a large number of branches, which not only leads to low efficiency, but also occupies a large amount of memory space. Therefore, based on the above algorithms, scholars have make some research on RRT algorithm from the aspects of sampling and expansion strategy. In terms of sampling strategies, the paper (Biao and Cao, 2021; Khan, 2020) adopted target paranoia to achieve "de-randomness." But this strategy only reduced a small amount of the redundant sampling. Therefore, to further reducing the sampling space, Liu et al. (2020), Chi et al. (2022) and Ganesan and Natarajan (2021) set the sampling interval of the traditional RRT algorithm in different ways to make the search more efficient. On the aspect of the extension strategy, the paper (Zhang et al., 2019; Wang et al., 2020; Kang et al., 2016; Kang, 2019; Khan, 2020) fused the RRT algorithm with APF algorithm. Specifically, it used the attractive action to guide the production of new nodes and improve the search speed of the algorithm. In this process, although the target attraction is introduced, the repulsion of obstacles is not considered, so the role of the APF algorithm cannot be fully simulated. Wang et al. (2022), Kabutan and Nishida (2018) get new nodes by the guiding effect of target gravity and obstacle repulsion. It improved not only the goal orientation but also the obstacle avoidance ability. But with the disadvantages of unreachable target and local minima, the APF algorithm made the RRT algorithm unable to find new sampling points in some cases (Yin et al., 2018). Therefore, a path planning algorithm with strong stability, high efficiency and strong generalization ability is urgently needed for the characteristics of high latitude and complex collision detection process of industrial robots.

To get more improvement on the adaptability and stability of the path planning algorithm, an APCS algorithm is proposed, which combines the efficient search and optimization ability of the improved APF algorithm with the completeness of the RRT algorithm. And it fundamentally solves the problem of environment adaptability and redundant sampling. Contributions of this paper are summarized as follows:

- An environment complexity function is proposed to make path planning algorithm adapt to the environment;
- An optimal sampling strategy is proposed, which not only makes full use of environmental information, but also considers the optimality of sampling points;
- A field cooperative expansion strategy is proposed, in which the improved APF algorithm is proposed and guides the generation of new nodes;

 A new algorithm called AFCS is proposed, which not only enhances the environmental adaptability of industrial robots, but also improves sampling quality and scaling efficiency of the path planning algorithm. The whole algorithm provides ideas for improving the intelligence of the path planning algorithm.

The rest of this article is arranged as follows: The principle of path planning of robots is analyzed, and the principle of the traditional path planning algorithm is introduced in section 2. Then the AFCS algorithms is introduced in section 3. Section 4, summary and analysis.

### 2 Materials and models

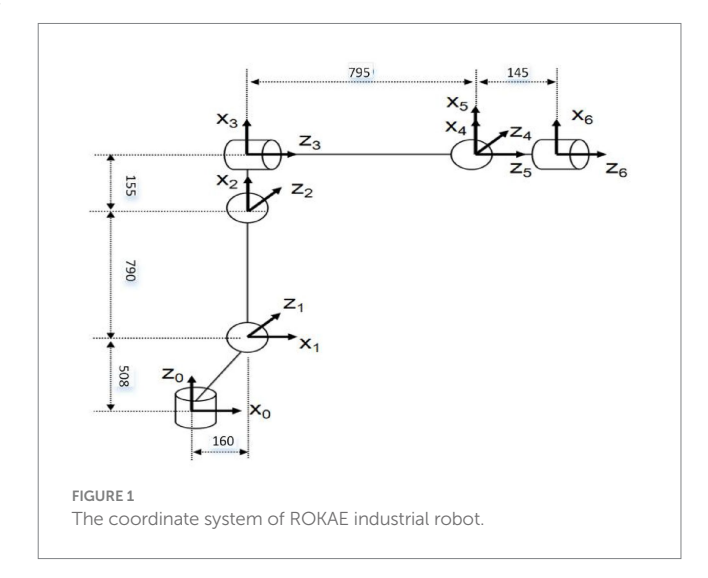
For industrial robots, it is a prerequisite for path planning to satisfy constraints in terms of kinematics and dynamics. In this article, the relevant theories of industrial robot path planning are further studied based on the full study of the kinematics of industrial robots.

### 2.1 Kinematic model of manipulators

Path planning of industrial robot needs mutual transformation in joint space and Cartesian space. So it involves the solution of inverse kinematics. And the accuracy of the inverse kinematics solution also certainly affects the accuracy of path planning of industrial robots. In this paper, ROKAE 6-DOF industrial robot is taken as the research object, and the coordinate system is established according to the DH model (Hartenberg et al., 1964) as shown in Figure 1.

Based on the homogeneous coordinate transformation matrix, the position and pose of the two adjacent coordinate systems i, i-1 of the industrial robot are obtained as follows:

$$\frac{i-1}{i}T = \begin{bmatrix}
\cos\theta_i & -\sin\theta_i\cos\alpha_i & \sin\theta_i\sin\alpha_i & a_i\cos\theta_i \\
\sin\theta_i & \cos\theta_i\cos\alpha_i & -\cos\theta_i\sin\alpha_i & a_i\sin\theta_i \\
0 & \sin\alpha_i & \cos\alpha_i & d_i \\
0 & 0 & 0 & 1
\end{bmatrix}$$
(1)



 $\theta_i$  represents the angle between the X axes of adjacent coordinate systems,  $\alpha_i$  represents the Angle between the Z axes of adjacent coordinate systems,  $a_i$  is the length of the common perpendicular of the Z axis,  $d_i$  is the distance between  $a_i$  and  $a_{i-1}$ .

According to the DH method, it is easy to get the forward kinematics equation of the industrial robot as follows:

$${}_{6}^{0}T = {}_{1}^{0}T {}_{2}^{1}T {}_{3}^{2}T {}_{4}^{3}T {}_{5}^{4}T {}_{6}^{5}T = \begin{bmatrix} n_{x} & o_{x} & a_{x} & p_{x} \\ n_{y} & o_{y} & a_{y} & p_{y} \\ n_{z} & o_{z} & a_{z} & p_{z} \\ 0 & 0 & 0 & 1 \end{bmatrix}$$
(2)

Where,  ${}^{i-1}\!IT$  represents the homogeneous transformation matrix of adjacent coordinate systems. According to the principle of forward kinematics, the position and attitude of the industrial robot can be solved according to Equation 2. The inverse kinematics solution is the inverse process of the forward kinematics solution. In the path planning of industrial robots, forward and inverse kinematics can be calculated as needed. The DH parameters of the ROKAE industrial robot used in this paper are shown in Table 1.

## 2.2 Path planning and model of environment

### 2.2.1 Path planning

The core of path planning is planning, and its goal is to obtain a path that satisfies the conditions. The path is a continuous curve in the configuration space of robots. Specifically, path planning may be to plan a non-collision and shortest path for mobile robots in two-dimensional space. It also can plan a safe, non-collision or relatively optimized path for industrial robots (as shown in Figure 2). Jiang Xinsong, the father of Chinese robots, defines path planning as follow: The goal of path planning is to get a non-collision path in the environment with obstacles according to certain evaluation criteria (Hong et al., 2022). Deservedly, the different distribution of obstacles in the environment directly affects the planned path, and the target location determination is provided by the higher-level task decomposition module (Hong et al., 2022).

### 2.2.2 Model of environment

In traditional path planning, environment modeling is the first step of path planning in order to better satisfy configuration space

TABLE 1 The DH parameters of the ROKAE industrial robot.

i	$d_i(mm)$	$\alpha_i(\deg)$	$a_i(mm)$	$\theta_i(\deg)$	
1	508	-90	160	$\theta_1$	
2	0	0	790	$\theta_2$	
3	0	-90	155	$\theta_3$	
4	795	90	0	$\theta_4$	
5	0	-90	0	θ5	
6	145	0	0	$\theta_6$	

constraints. However, it is more and more difficult to model the environment in the more complex scenario. The complexity of environment modeling is an important problem that restricts the path planning of robots. This article puts forward the environmental complexity function to counter the difficulty of environment modeling. This strategy realizes the prediction of the environment where the path planning is located, and lays a theoretical foundation for path planning algorithm to take full advantage of the environmental information. This paper designs two kinds of environment maps (as shown in Figure 3), in which the superiority of path planning algorithm can be better reflected.

As shown in Figure 3, the number of obstacles in two maps is the same, but the complexity of the environment is different because of the different distribution of obstacles. The pixel size of the two maps is1500\*1500. In this paper, the starting point position coordinate of path planning is (0, 0, 0), and the target point coordinate is set to (1000, 1000, 1000).

### 2.3 Path planning algorithm

The sampling-based RRT algorithm and APF algorithm are the most widely used in path planning of industrial robots. By fully studying the traditional APF algorithm and RRT algorithm, this article summarizes the advantages and disadvantages of the two methods. At the same time, this article makes same improvement of the traditional algorithms in view of their shortcomings, and a new AFCS algorithm with strong environment adaptability is proposed.

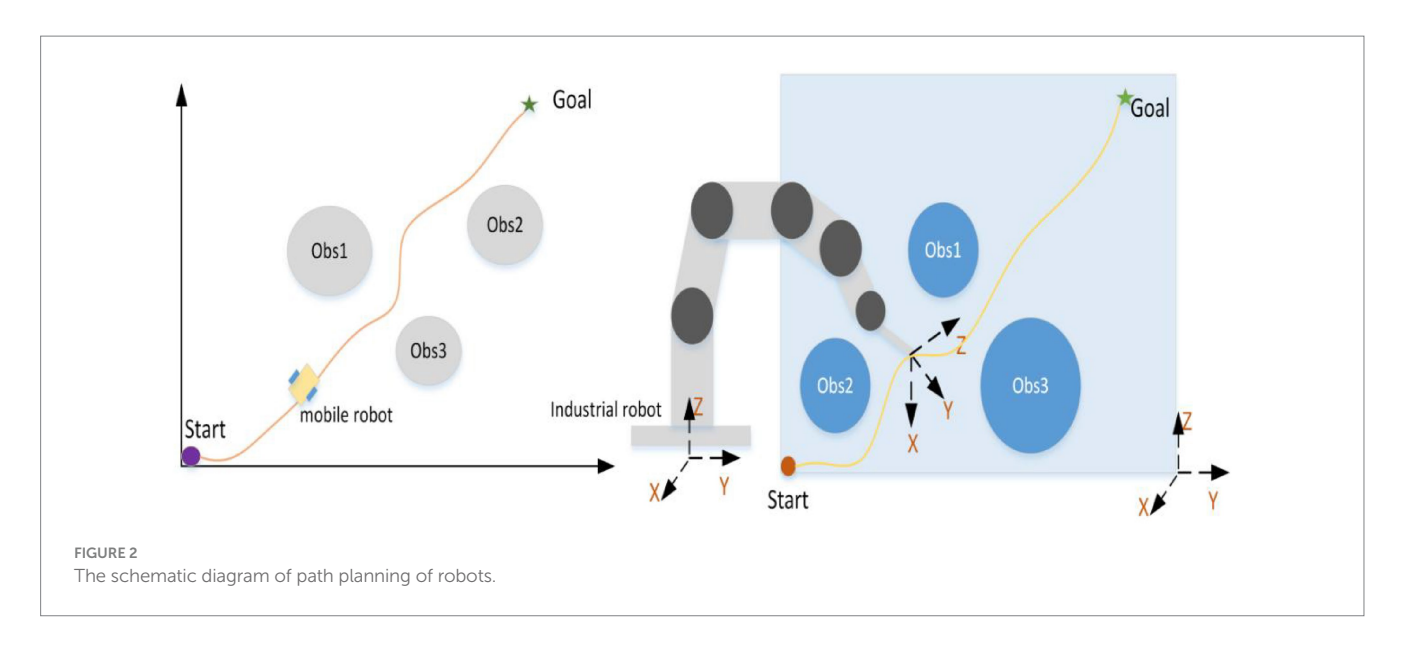
### 2.3.1 RRT algorithm

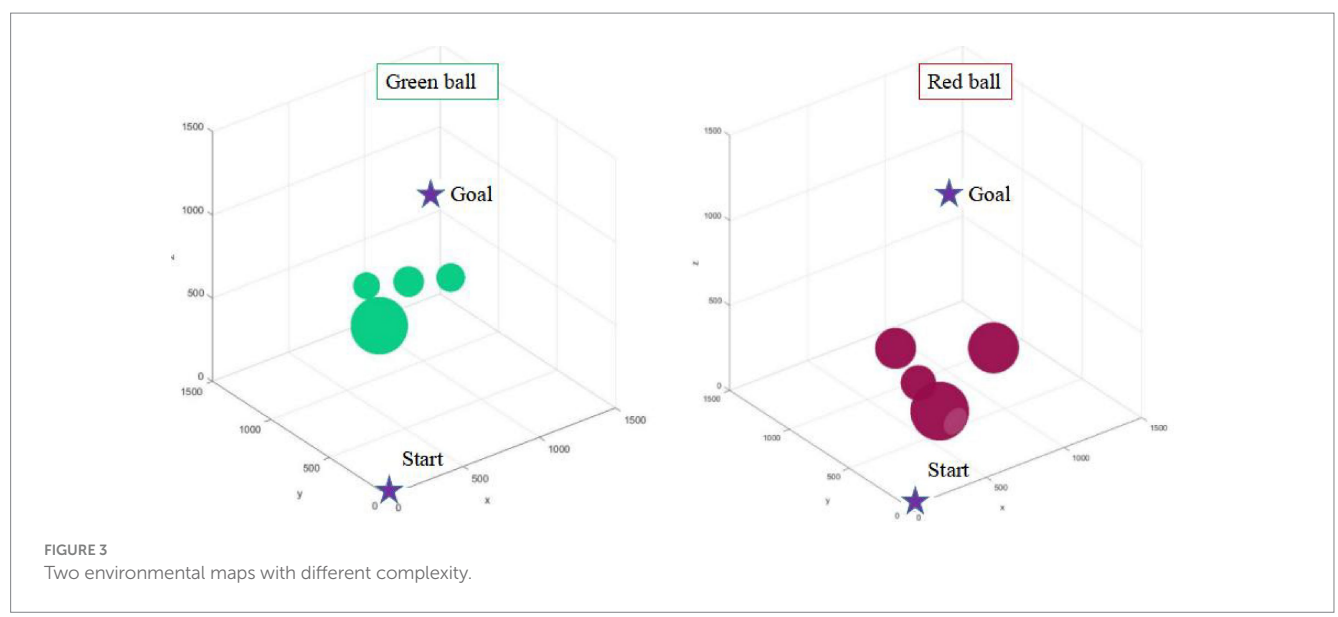
There is a path search algorithm called the RRT algorithm, which expands by random sampling. It establishes the search tree from the starting point. Subsequently, it undergoes random sampling, expands new nodes, avoids obstacles, and finally finds an optimal path. Figure 4 shows the implementation process of the traditional RRT algorithm, and its pseudo-code is shown in Figure 5.

The core of traditional RRT algorithm can be divided into four stages: sampling, expansion, collision detection and path query. There are three important factors that lead to the low efficiency and poor applicability of RRT algorithm, which are the redundant sampling in the sampling phase, the way and efficiency of generating new nodes in the expansion phase, and the amount of calculation in collision detection (Junxiang and Wang, 2021). Especially in the sampling stage, the redundant sampling not only has strong randomness, but also does not consider the optimality of sampling. Moreover, in the measurement connection stage, the generation of new nodes is neither guided nor considering the influence of obstacles, so that the calculation of collision detection of the RRT algorithm is very large. Generally, the randomness and efficiency of the RRT algorithm are important factors affecting its development. Therefore, this paper proposes an efficient RRT algorithm to solve the strong randomness and low efficiency.

#### 2.3.2 APF algorithm

The APF algorithm is a simple and effective local path planning algorithm. It constructed by Dr. Oussama Khatib who introduced the concept of "field" in traditional mechanics (Fan et al., 2020; Rostami, 2019). The potential field includes the attractive and repulsive





potential field, which are formed by the target and the obstacle, respectively. The agent moves along the resultant force of the attractive and repulsive forces (Yuan et al., 2021). The attractive and repulsive potential field functions are modeled as follows

$$U_{att}\left(P\right) = \frac{1}{2}k_t \left\| P - P_{goal} \right\| \tag{3}$$

$$U_{rep}(P) = \begin{cases} 0 & dP || -P_{obs} || \ge D_2 \\ \frac{k_r}{2} \left( \frac{1}{||P - P_{obs}||} - \frac{1}{D_2} \right) & dP - ||P_{obs}|| < D_2 \end{cases}$$
(4)

Where,  $U_{att}\left(P\right)$  denotes the attractive potential field of the node  $P, k_t$  is the attractive coefficient.  $||P-P_{goal}||$  denotes the distance between two nodes P and  $P_{goal}$ ; The repulsive potential field generated

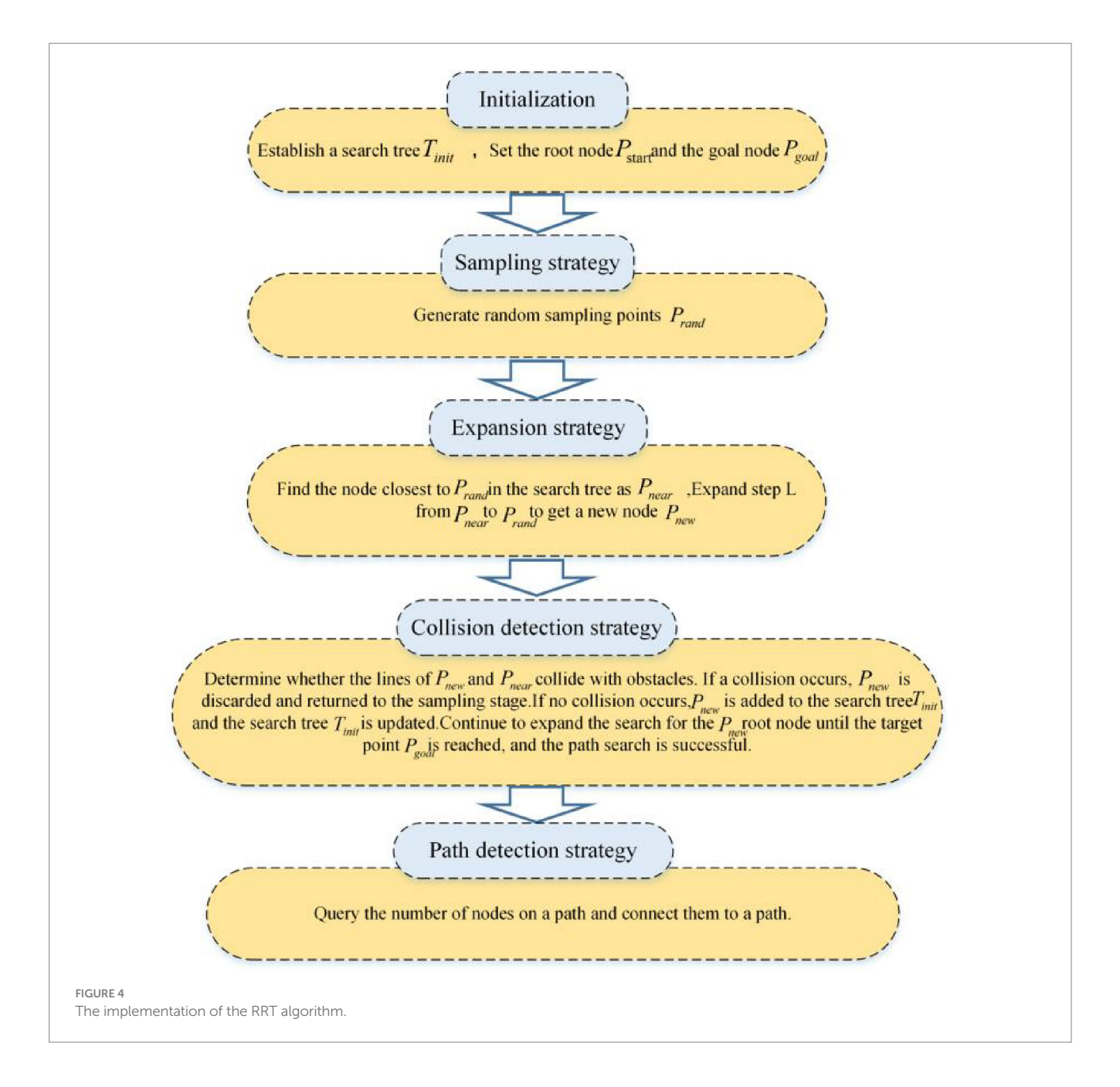
by the node P is expressed as  $U_{rep}(P)$ ,  $k_r$  is the repulsion coefficient;  $||P-P_{obs}||$  denotes the distance between two nodes P and  $P_{obs}$ ,  $D_2$  indicates the influence threshold of an obstacle; When  $||P-P_{obs}|| \ge D_2$ , the node is not affected by obstacles; When  $P-P_{goal} < D_2$ , the node is affected by the repulsive potential field of the obstacle.

The model of the attractive and repulsive forces are shown as follow:

$$F_{att}(P) = -\Delta U_{aat}(P) = k_t || P - P_{goal} ||$$
(5)

$$F_{rep}(P) = -\Delta U_{rep}(P) =$$

$$\begin{cases}
0 & d || P - P_{obs}|| \ge D_2 \\
-k_r \left( \frac{1}{|| P - P_{obs}||} - \frac{1}{D_2} \right) & d || P - P_{obs}|| < D_2
\end{cases}$$
(6)



The resultant force of attraction and repulsion is shown as follow:

$$F_{total}(P) = F_{att}(P) + F_{rep}(P) \tag{7}$$

The agent realizes obstacle avoidance path planning under the guidance of the resultant force, and its schematic diagram is shown in Figure 6.

On the basis of the principle of the APF algorithm, it can be known that the magnitude of the attraction and repulsion force of the agent are related to the corresponding distance. So its main disadvantages are the inaccessible target and local minimum (Wang et al., 2022). Otherwise, the essence of the APF algorithm is a control method, and its path is generated by the control quantity in real time. Therefore, its real-time performance is more strong. For the shortcomings of the APF algorithm, this paper proposes an improved

APF algorithm, and introduces it into the traditional RRT algorithm to improve its real-time performance.

# 2.4 The adaptive field cooperative sampling algorithm

On the principle of path planning algorithm, this paper innovatively put forward an adaptive field cooperative sampling algorithm. Firstly, the environment complexity function is proposed for the difficulty of environment modeling. Then, an improved APF algorithm is proposed to solve the inaccessible target and local minimum. Finally, based on the framework of the traditional RRT algorithm, an optimal sampling strategy is proposed, and the AFCS algorithm is obtained by introducing the environment complexity function and the improved APF algorithm into the RRT algorithm.

```
Algorithm 1: Basic RRT
    Input:
              Initial configuration p<sub>start</sub> p<sub>goal</sub> S<sub>obs</sub>
              Number of sampling point K
              Step size \delta
    Output:
              Search tree T
             Vertices of path V
         Initialize all Parameters;
         T = p_{\text{start}};
         for i = 1 to K do
    3.
              p<sub>rand</sub>=Sample();
    4.
              p_{near} Nearest (nodes, p_{rand});
              p_{\text{new}} \leftarrow \text{Steer}(p_{\text{near}}, p_{\text{rand}}, \delta);
             if CollisionFree(p<sub>near</sub>,,p<sub>new</sub>)then
    7.
                 T.add(p_{new});
                 return Advanced;
             if d (p_{new}, p_{goal}) < Error then
    10.
                return Reached;
    11.
            else
    12.
                continue;
    13.
         final;
    14.
         return T&V;
FIGURE 5
The pseudo-code of the traditional RRT algorithm
```

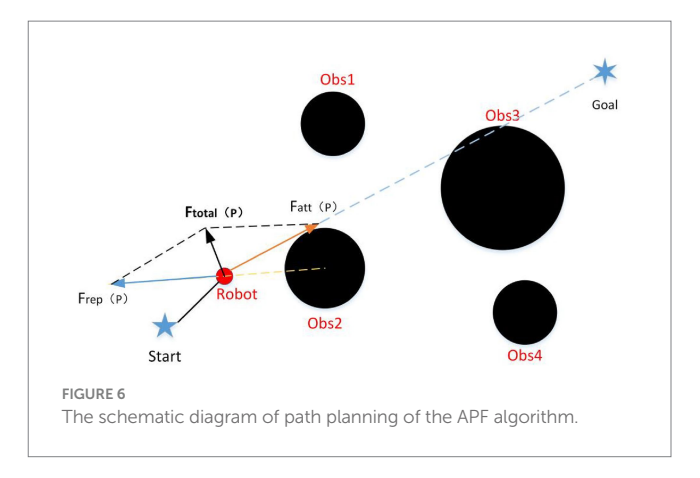
### 2.4.1 Environment complexity function

Aiming at the complex of environment modeling, this article designs the environment complexity function *S* based on the relative position of obstacles in the environment. Then it is introduced into the traditional RRT algorithm. This operation enables the algorithm to intelligently adjust the iteration time instead of manually adjusting the iteration parameters according to the complexity of the environment. And it also improves its environmental adaptability. On the basis of the volume ratio of obstacles, this article introduces the distance between obstacles to further distinguish the complexity, so as to make the path planning algorithm suitable for environments with different complexity. The environment complexity function is as follows:

$$S = \lambda_1 \frac{n_1 V_{obs_1} e^{10}}{V L^3} \tag{8}$$

Where, S represents the environment complexity.  $n_1$  respectively indicates the number of static in the environment (Urain et al., 2023).  $V_{obs1}$  represents the volume of static obstacles. V represents the total volume. Only one class of static obstacle cases is studied here, so  $\lambda_1 = 1$ .

According to the proposed environment complexity function, the environment complexity of the two maps in Figure 4 can be, respectively, calculated as: 2301, 1809. Although the number of obstacles in the two maps is the same, the relative position of obstacles is different. In the green sphere environment, the minimum distance between obstacles is 697 mm. In the red sphere environment, the



minimum distance between obstacles is 883 mm. The green sphere environment is relatively complex. Therefore, the design of the environment complexity function is reasonable.

### 2.4.2 Optimal sampling strategy

For the RRT algorithm and its variants, the ideal sampling procedure is one that reduces redundant sampling while keeping the sampling point on or near the optimal path as much as possible. Based on the above ideas, this article proposes an optimal sampling strategy to solve redundant sampling and poor quality of sampling points in the sampling stage. The idea of this strategy is to randomly generate multiple sampling points at the same time, and then determine the sampling quality function based on the density of obstacles around the sampling points and the smoothness of the path. In this way, random sampling points with optimal quality can be obtained. The sampling quality function is modeled as follows:

$$M_{P_{nandi}} = w_1^* \rho_{P_{randi}} + w_2^* \sigma_{P_{randi}} \tag{9}$$

$$P_{randi} = \frac{\max ||P_{randi} - P_{obs}||}{A}$$
 (10)

$$\sigma_{randi} = \frac{\angle P_{randi} P_{nearest} P_{k-1}}{180^{\circ}}$$
 (11)

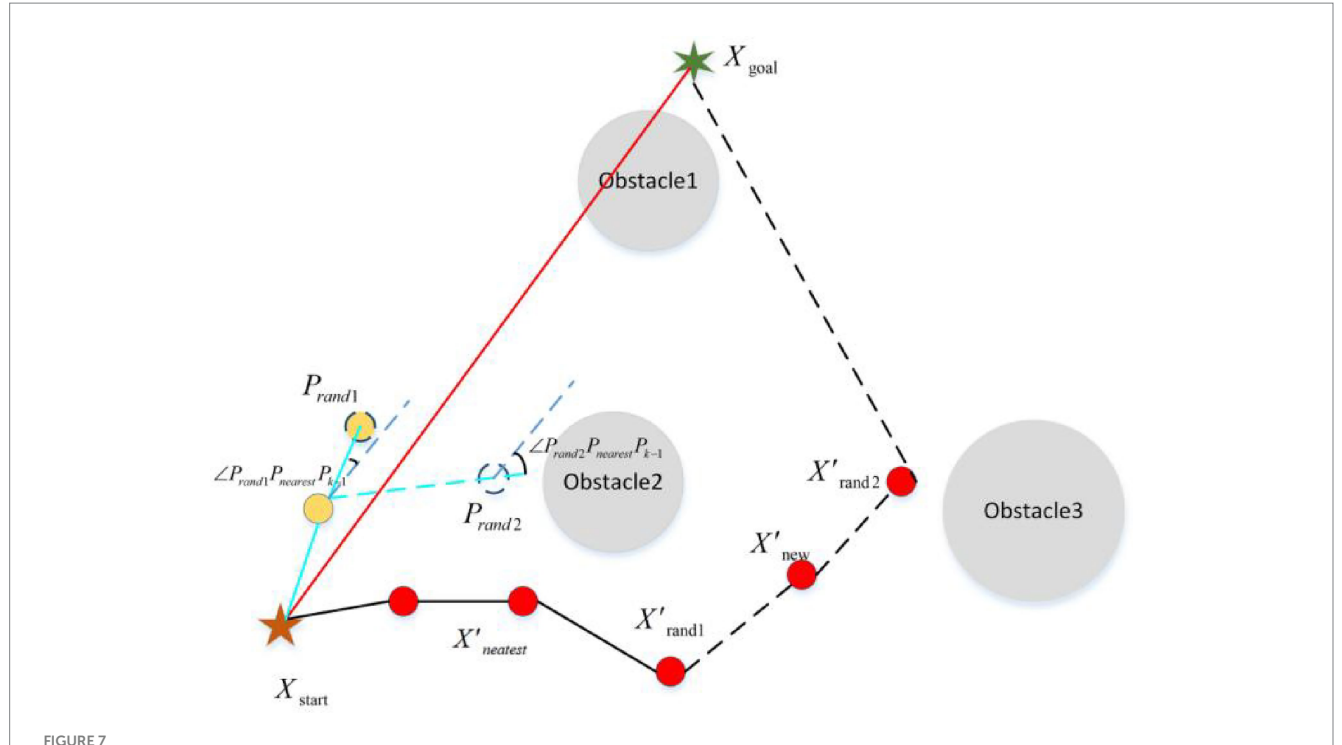
Where,  $M_{P_{nundil}}$  represents the quality function of the i random sampling point  $P_{randi}$ .  $\rho_{P_{rundil}}$  is the density of obstacles around the random sampling point  $P_{randi}$ .  $\sigma_{P_{nundil}}$  represents the smoothness of the random sampling point  $P_{randi}$ .  $||P_{randi}-P_{obs}||$  represents the distance between the random sampling point  $P_{randi}$  and the nearest obstacle  $P_{obs} \angle P_{randi} P_{nearest} P_{k-1}$  represents the angle between the line  $P_{randi} P_{nearest}$  and  $P_{nearest} P_{k-1} w_1$ ,  $w_2$  represent the influence factors of obstacle density and smoothness of sampling points.

The schematic diagram of optimal sampling process is shown in Figure 7.

### 2.4.3 Field cooperative expansion strategy

### 2.4.3.1 The improved APF algorithm

For the problem of the inaccessible target and local minimum, this article, respectively, introduces the distance between the target point and the robot into the attractive potential field and the repulsive



The schematic diagram of optimal sampling process (the blue path represents the optimal sampling process, and the black path represents the path generated by the random sampling process).

potential field function of the traditional APF algorithm. Based on papers (Ahmadi et al., 2022; Guo et al., 2022), the attractive and repulsive potential field models proposed in this paper are shown as follow:

$$U_{att}(P) = \begin{cases} \frac{k_t || P - P_{goal} ||}{2} & d || P - P_{goal} || \le D_1 \\ D_1 k_t || P - P_{goal} || - \frac{k_t D_1^2}{2} & d || P - P_{goal} || > D_1 \end{cases}$$
(12)

$$U_{rep}(P) = \begin{cases} 0 & d || P - P_{obs}|| \ge D_2 \\ \frac{k_r}{2} \left( \frac{1}{||P - P_{obs}||} - \frac{1}{D_2} \right) - \frac{1}{2} \sigma || P - P_{goal} || & d || P - P_{obs} || < D_2 \end{cases}$$
(13)

Where,  $U_{att}\left(P\right)$  represents the attractive potential field,  $k_t$  is the attractive coefficient.  $||P-P_{goal}||$  denotes the distance between two nodes Pand t  $P_{goal}$ .  $D_1$  represents the threshold for the node to reach the target point. When  $||P-P_{goal}|| \leq D_1$ , the robot approaches the target point at a faster speed. Otherwise, the robot approaches the target point at a slower speed.  $U_{rep}\left(P\right)$  represents the repulsive potential field.  $k_r$  is the repulsion coefficient.  $||P-P_{obs}||$  denotes the distance between two nodes P and  $P_{obs}$ ,  $D_2$  indicates the influence threshold of an obstacle.  $\sigma$  represents the distance influence factor. When  $||P-P_{obs}|| \geq D_2$ , the node is not affected by obstacles; When  $||P-P_{goal}|| < D_2$ , the repulsive potential field of the obstacle dose not work.

The attractive and repulsive function models are shown as follows:

$$F_{att}\left(P\right) = \begin{cases} k_t \mid\mid P - P_{goal} \mid\mid & d \mid\mid P - P_{goal} \mid\mid \leq D_1 \\ D_1 \cdot k_t \cdot \mid\mid P - P_{goal} \mid\mid -k_t \cdot D_1 & d \mid\mid P - P_{goal} \mid\mid > D_1 \end{cases} \tag{14}$$

$$\begin{cases} F_{rep}(P) = \\ \begin{cases} 0 & d || P - P_{obs} || \ge D_2 \\ -k_r \left( \frac{1}{|| P - P_{obs} ||} - \frac{1}{D_2} \right) + \sigma || P - P_{goal} || & d || P - P_{obs} || < D_2 \end{cases} \end{cases}$$
(15)

In this paper, the field cooperative expansion strategy is to introduce the improved APF algorithm into the traditional RRT algorithm. The position and orientation of the new nodes are calculated according to the improved APF algorithm. The new node is calculated as follows:

$$P_{new} = P_{nearest} + \beta_1 P_{rand} + \beta_2 \frac{F_{total}(P)}{||F_{total}(P)||}$$
(16)

$$F_{total}(P) = F_{att}(P) + F_{rep}(P) \tag{17}$$

Where,  $P_{new}$  is the new node.  $P_{rand}$  represents the random sampling point, whose nearest point on the random tree is expressed as  $P_{nearest}$ .  $\beta_1$ ,  $\beta_2$  represents the influence factors of the random node and target gravity on the new node.  $F_{total}(P)$  represents the resultant force of the potential field.  $F_{att}(P)$  represents the sum of the attractive forces of the random node and the target node on the new node.  $F_{rep}(P)$  represents the sum of the repulsive forces of obstacles on new nodes.

The schematic diagram of field cooperative expansion strategy is shown in Figure 8.

### 2.4.4 The adaptive field cooperative sampling algorithm

Based on the above innovative strategy, an adaptive field co-sampling algorithm is proposed in this paper. It not only avoids complex environment modeling, but also makes full use of environment information. Moreover it solves the redundant sampling and low efficiency of traditional RRT algorithm by the optimal sampling strategy and the introduction of improved APF algorithm. The flow chart of the AFCS algorithm is shown in Figure 9.

The pseudo-code of the AFCS algorithm is shown in Figure 10.

integrates the AFCS algorithm with industrial robot simulation to verify its effectiveness and practicability.

In two maps with different complexity, this article conducts

In the aspect of industrial robot simulation, this paper mainly

In two maps with different complexity, this article conducts multiple simulation experiments with the same number of iterations and step size, respectively. The multiple operation results of the traditional RRT algorithm and RRT\* algorithm are shown in Figures 11, 12.

In Figures 11, 12, the RRT algorithm and RRT\* algorithm fail the path planning due to the large amount of redundant sampling in the tow environments. Although both RRT and RRT\* algorithms are probabilistic complete, such a time-consuming strategy is not desirable in practice. Therefore, this article focuses on the comparison and analysis of simulation results between the AFCS algorithm and the most representative tRRT algorithm.

### 3 Experiments and results

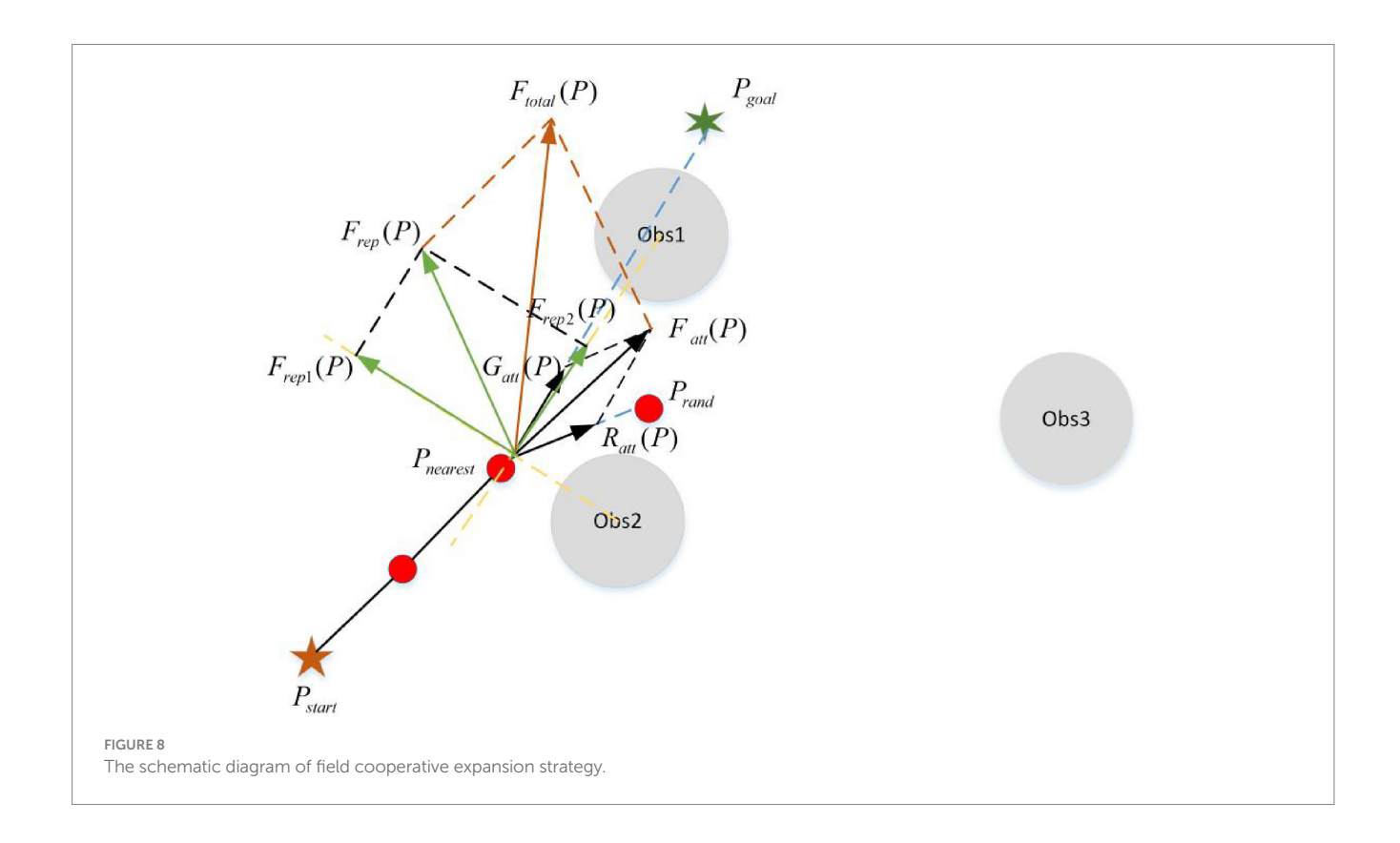
Simulation experiment is an important way to show the superiority of the algorithm. The simulation experiment in this paper is carried out in two aspects: algorithm simulation and industrial robot simulation.

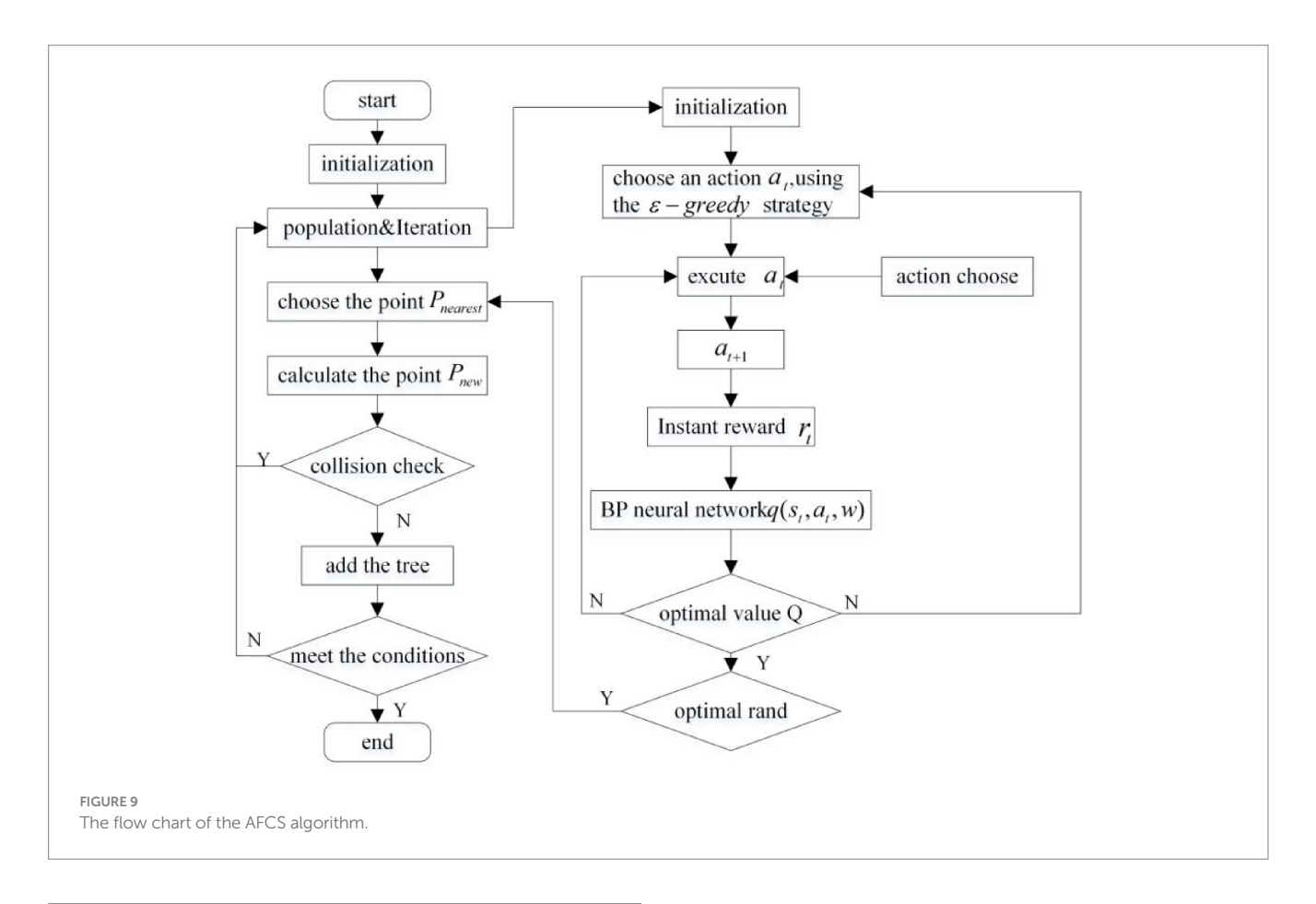
In terms of algorithm simulation, two environments with different complexity are used to carry out simulation experiments to verify the environmental adaptability of the algorithm. At the same time, this paper verifies the effectiveness and practicability of the AFCS algorithm by analyzing the experimental results with the traditional RRT algorithm, RRT\* algorithm and tRRT algorithm from three aspects: planning time, path cost and the number of path points.

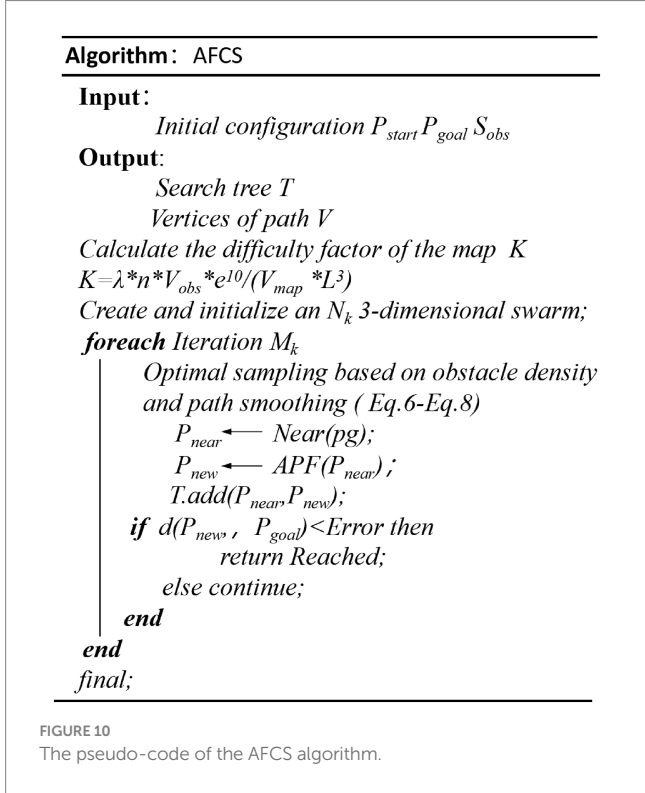
### 3.1 Experiment of algorithm simulation

### 3.1.1 Analysis of environmental adaptability

Environmental adaptability is an embodiment of the intelligence of path planning algorithm. It is also an important direction to improve the intelligence of industrial robots. Five consecutive simulation experiments are carried out in two environments with different complexity (as shown in Figures 13, 14) to verify the environmental adaptability of the algorithm. It should be noted that the number of iterations of the AFCS algorithm is related to the environment complexity function without manual mediation. The iteration and step size of the tRRT algorithm are the same.







It can be seen from Figures 13, 14 that the results of the AFCS algorithm are more stable. And the branches of the path obtained by the AFCS algorithm are less. But when the environment of the tRRT

algorithm changes (from red sphere environment to green sphere environment), the branches of its path becomes more and more. Therefore, the proposed AFCS algorithm has better adaptability to the environment and higher stability.

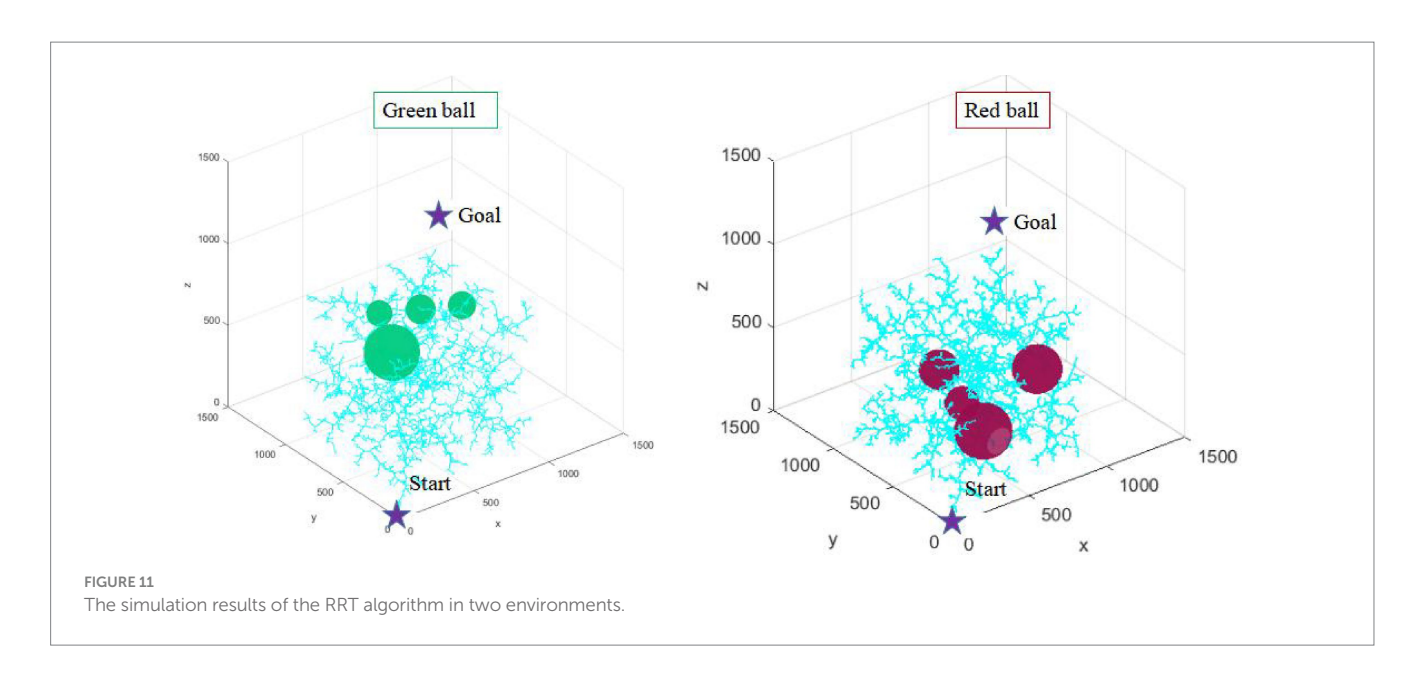
### 3.1.2 Analysis of efficiency

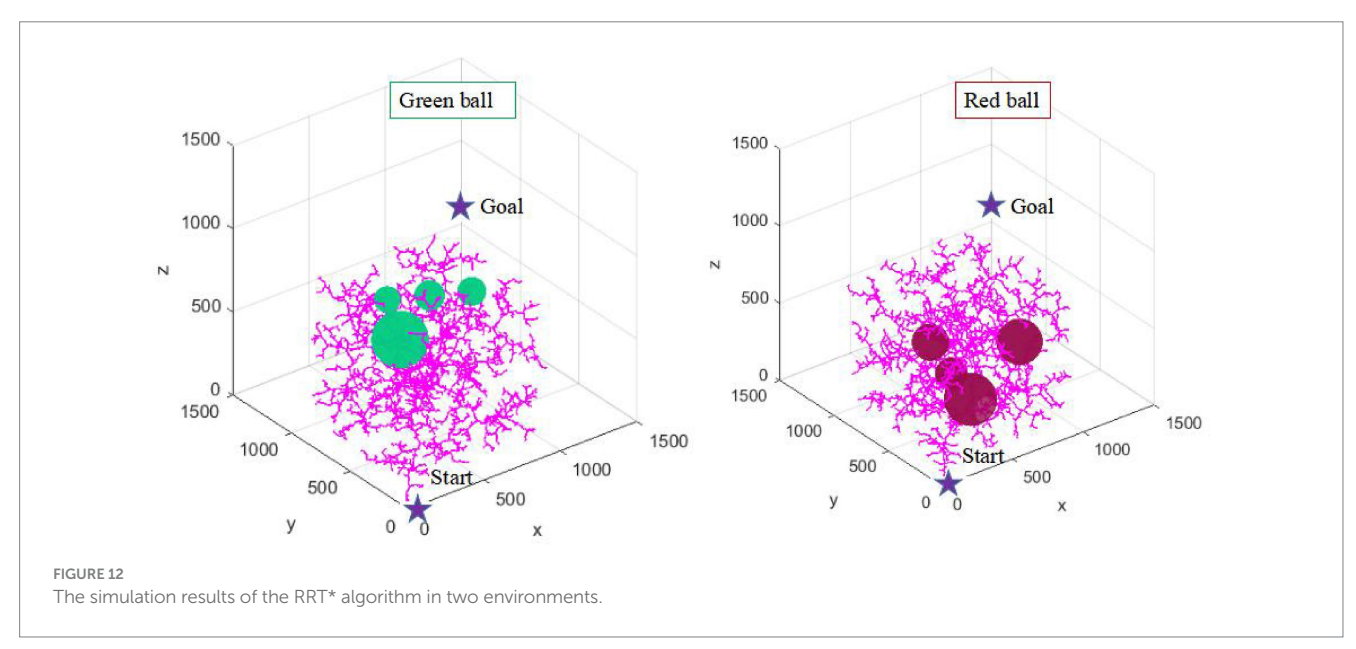
Time is an important reflection of efficiency. In this paper, the planning time of the algorithm in the same environment is taken as one of the criteria to measure the efficiency of the algorithm. The AFCS algorithm and tRRT algorithm are run 10 times in two environments with different complexity to obtain the average planning time of the algorithm (as shown in Table 2).

According to the data in Table 2, in the environment with different complexity, the planning time of the AFCS algorithm remains stable and does not float with the change of environment. In contrast, the efficiency of the tRRT algorithm fluctuates by about 27% as the complexity of the environment changes. This fluctuation of operating efficiency will affect the expansion of application scenarios of the algorithm. On the other hand, in the environment with the same complexity, the AFCS algorithm has shorter planning time and higher stability than the tRRT algorithm.

This paper runs the AFCS algorithm and the tRRT algorithm for 20 times, respectively, in the green sphere environment to further verify the stability of the AFCS algorithm. The path planning time of the two algorithms is shown in Table 3.

In Table 3, the planning time of 20 times of the AFCS algorithm is stable between 3.904~s-5.2919~s, and the planning time fluctuates little in the green sphere environment. However, the 20 times path planning time of tRRT algorithm fluctuates from 4.4478~s to 46.7573~s.





Therefore, the AFCS algorithm not only has high planning efficiency, but also has good stability.

### 3.1.3 Analysis of path quality

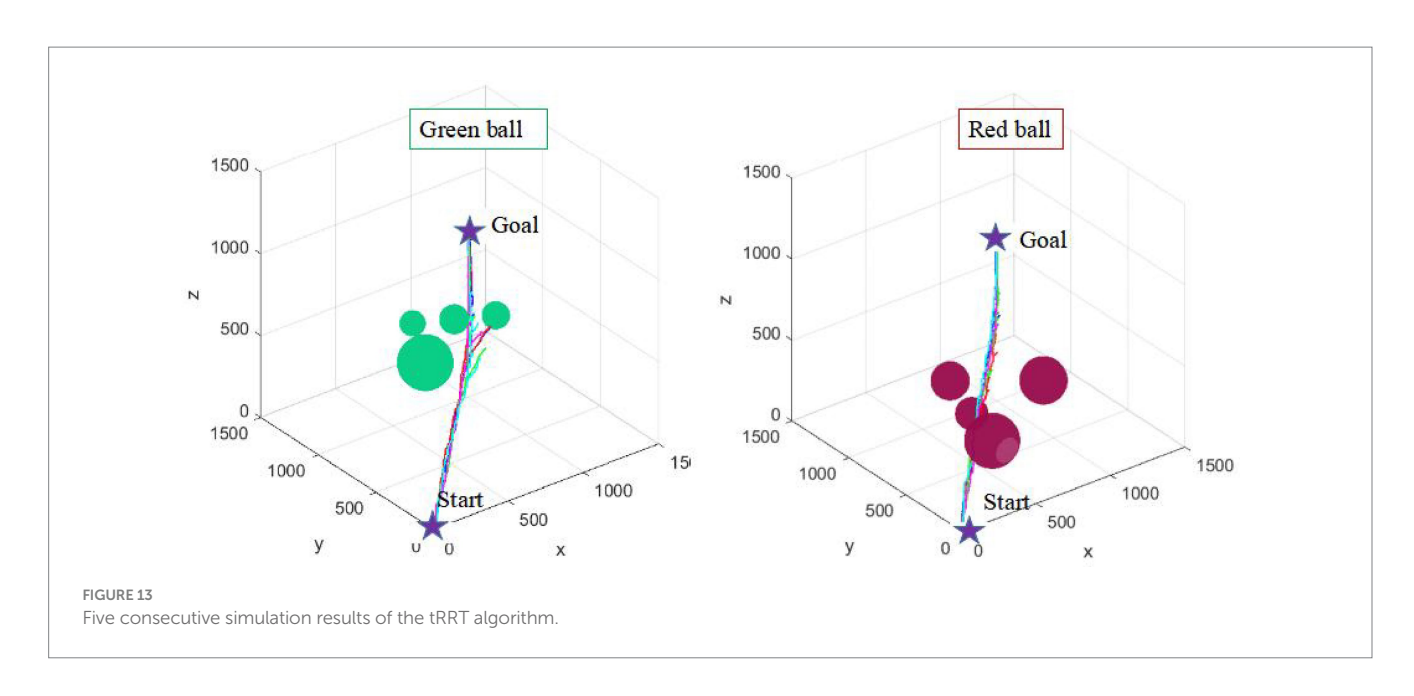
Path quality is an important factor to measure the planning efficiency of the algorithm. Path cost and the number of path nodes are important performances of path quality. In this paper, the sum of distance between nodes on the path is taken as the path cost. In this paper, the path cost obtained by running the AFCS algorithm and tRRT algorithm 5 times in two environments is shown in Figure 15.

In Figure 15, the path cost of the AFCS algorithm is about 20% smaller than that of the tRRT algorithm in the red sphere environment. In a more complex environment (green sphere environment), the path cost of the adaptive field co-sampling algorithm is about 50% less than that of the tRRT algorithm, which indicates that the path of the

adaptive field co-sampling algorithm is shorter. After running the algorithm 5 times, the path cost float of the AFCS algorithm is smaller than that of the tRRT algorithm, which indicates that the AFCS algorithm has better stability.

In this paper, the AFCS algorithm and tRRT algorithm were run five times, respectively, in two environments, and the number of path nodes was obtained, as shown in Figure 16.

In Figure 16, the number of path nodes planned by the AFCS algorithm for five times is also smaller than that of the tRRT algorithm in the red sphere environment, and the number of nodes decreases within a range of 2–5%. In the green sphere environment, the advantage of the adaptive field co-sampling algorithm is more obvious, and the reduction interval of the number of path nodes for 5 times is 21.1–50%. For different complex environments, the number of path nodes of the AFCS algorithm fluctuates little, ranging from 1.4 to 5.4%.



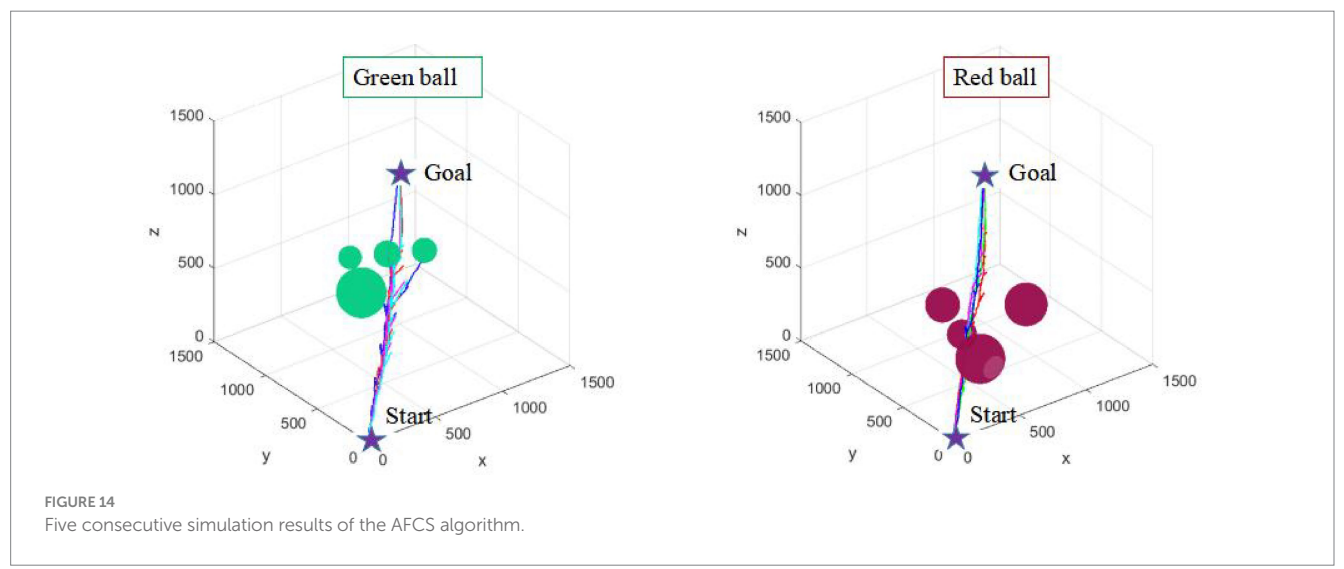


TABLE 2 The planning time of the AFCS algorithm and tRRT algorithm.

i	Greer	n Ball	Red Ball			
	AFCS	tRRT	AFCS	tRRT		
1	4.8414	7.4142	4.7543	4.4731		
2	4.5426	5.9894	4.3211	4.9958		
3	4.5295	5.2871	4.4687	4.3985		
4	3.8931	6.4891	4.3451	4.6828		
5	4.6952	5.3633	4.2883	4.1987		
AVE	4.5004	6.1086	4.4355	4.5498		

### 3.2 Experiment of industrial robot

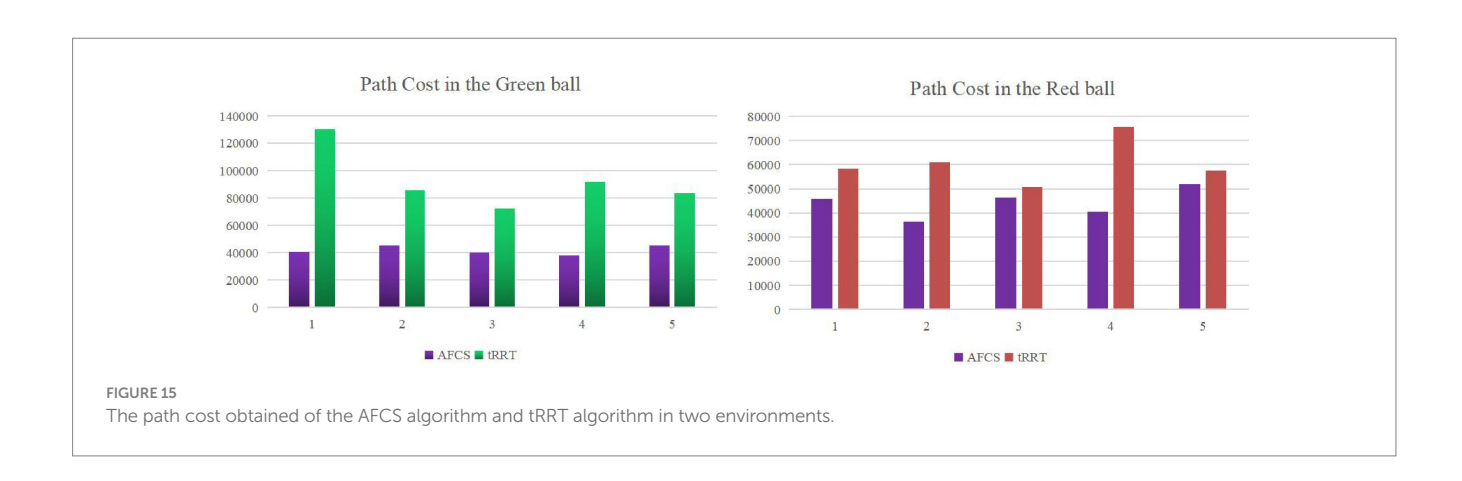
In order to verify the practicability of the algorithm, the path planning simulation experiment is carried out combining the AFCS algorithm with ROAKE industrial robot XB20 in the green sphere environment. The whole system of the path planning experiment is composed of computer, ROKAE industrial robot XB20 and ZED2 depth camera. Among them, the communication and logical relationship of the three hardware devices are shown in Figure 17.

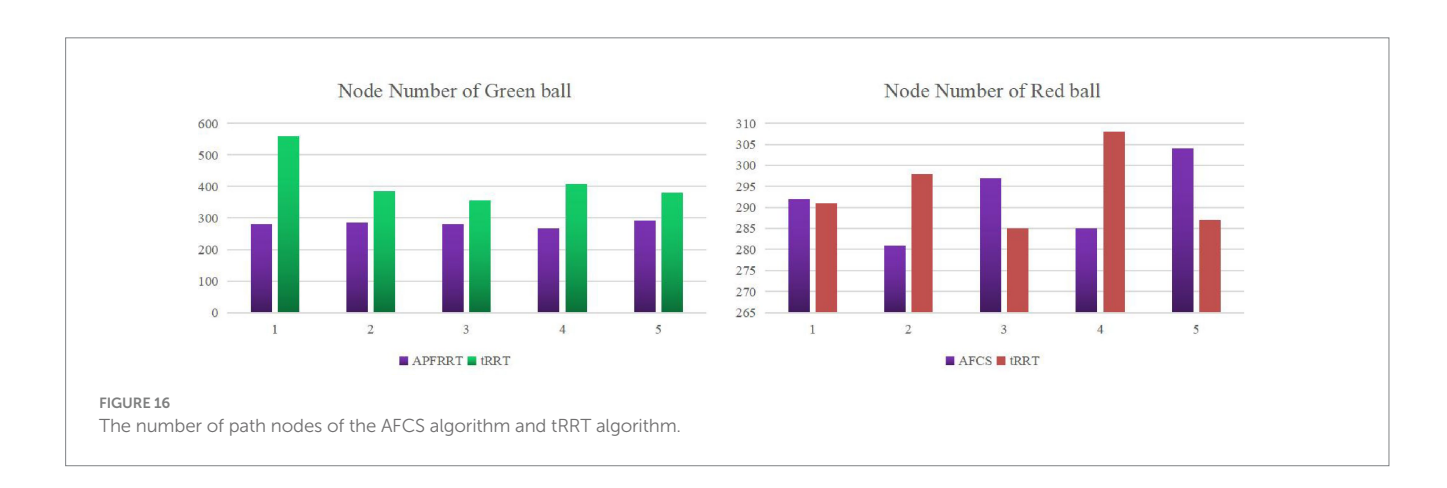
Based on the above hardware devices, the experimental flow is shown in Figure 18. The whole process of the experiment consisted of three parts (as shown in Figure 18). The first one is obstacle recognition based on ZED2 depth camera, which mainly obtains the position of obstacles for path planning of industrial robots. The second is path planning based on adaptive field cooperation, which mainly obtains collision-free paths of industrial robots. The third is to control the operation of industrial robots based on collision-free paths (Table 4).

Specifically, the experimental steps and the results of key steps are as follows:

1 The information of the experiment scene can be obtained by the depth camera. And the 3D coordinates of obstacles in the

L D G G	No	1	2	3	4	5	6	7	8	9	10
	Time (s)	5.593	47.252	5.336	26.35	5.739	19.945	6.995	40.209.506	12.134	19.228
AFCS	No	11	12	13	14	15	16	17	18	19	20
	Time (s)	16.58	18.991	7.135	23.16	4.899	32.178	36.55	15.46	18.733	4.976
tRRT	No	1	2	3	4	5	6	7	8	9	10
	Time (s)	3.804	3.9724	4.1898	4.753	4.298	4.2431	4.4561	4.5607	4.569	4.145
	No	11	12	13	14	15	16	17	18	19	20
	Time (s)	4.235	4.1579	4.3760	4.409	4.3345	4.4708	4.4809	4.3547	4.6079	5.1245





industrial robot coordinate system can be obtained by binocular camera calibration and hand-eye calibration.

The results of hand-eye calibration are shown in Equation 18:

$$X = \begin{bmatrix} 0.9976 & -0.0196 & -0.0668 & 16.7035 \\ 0.0222 & 0.9990 & 0.0389 & 6.4285 \\ 0.0660 & -0.0403 & 0.9970 & 108.3157 \\ 0 & 0 & 0 & 1.0000 \end{bmatrix}$$
 (18)

- 2 Based on the three-dimensional coordinates of obstacles, the path planning is carried out by the adaptive field co-sampling algorithm, and the Angle values of each joint of the industrial robot are obtained based on the inverse kinematics solution method.
- 3 The time series of six joint angles of industrial robot is obtained by using the trajectory planning algorithm (7th degree polynomial trajectory planning algorithm).
- 4 Socket software is used to send the joint Angle value of the industrial robot to ROKAE industrial robot XB20 to control the movement of it.

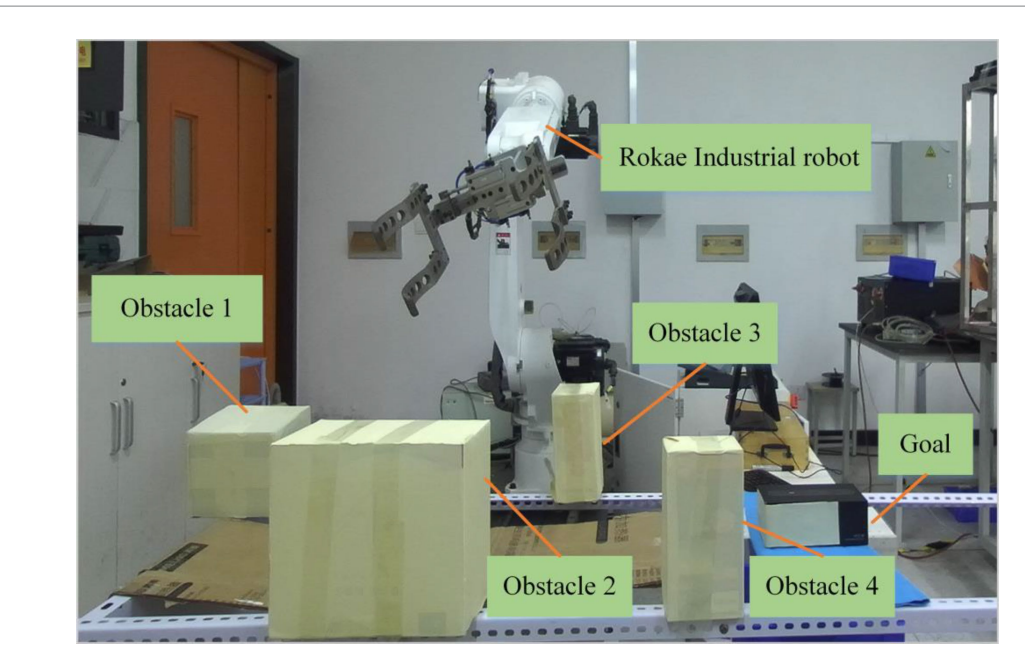
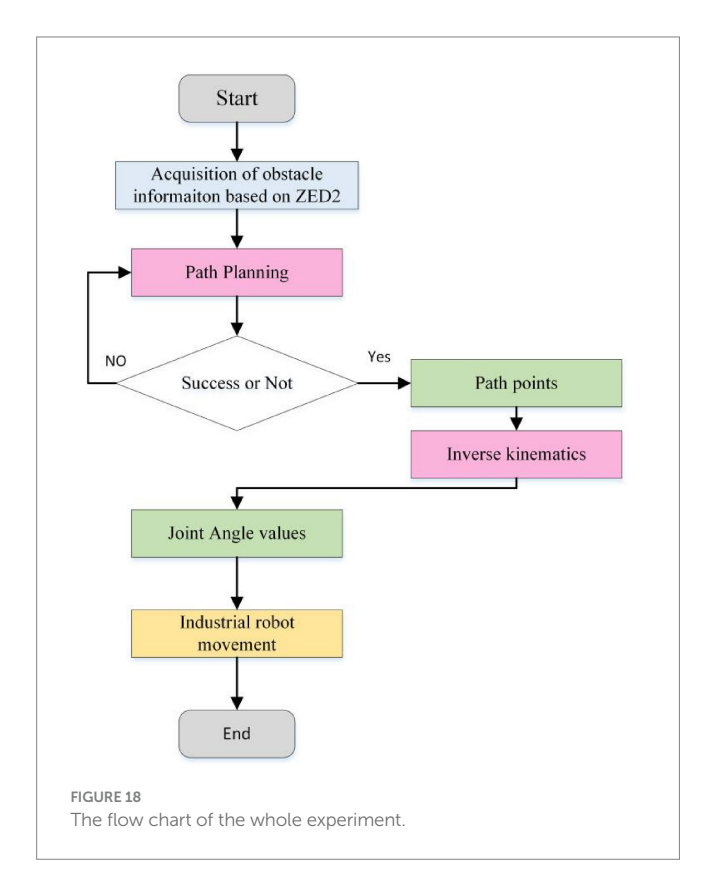


FIGURE 17
The communication and logical relationship of the three hardware devices



During the planning process, the Angle changes of the six joints of ROKAE industrial robot XB20 are shown in Figure 19.

The joint Angle velocity curve of 6 joints of path planning based on adaptive field cooperative sampling path planning algorithm is shown in the Figure 20.

It can be seen from the change curve of joint Angle value of industrial robots in Figure 20, the adaptive field cooperative sampling

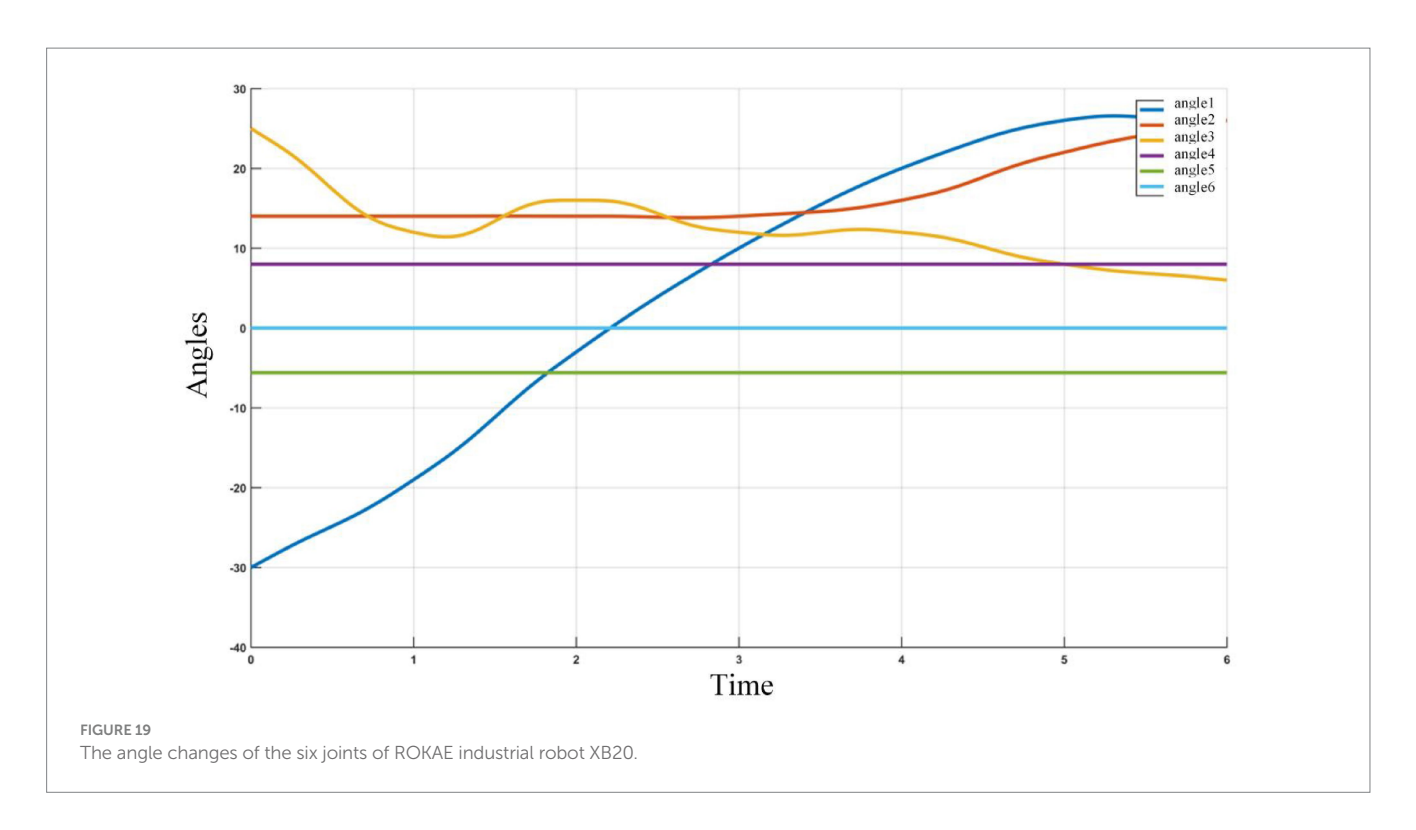
TABLE 4 The result of calibration of binocular camera.

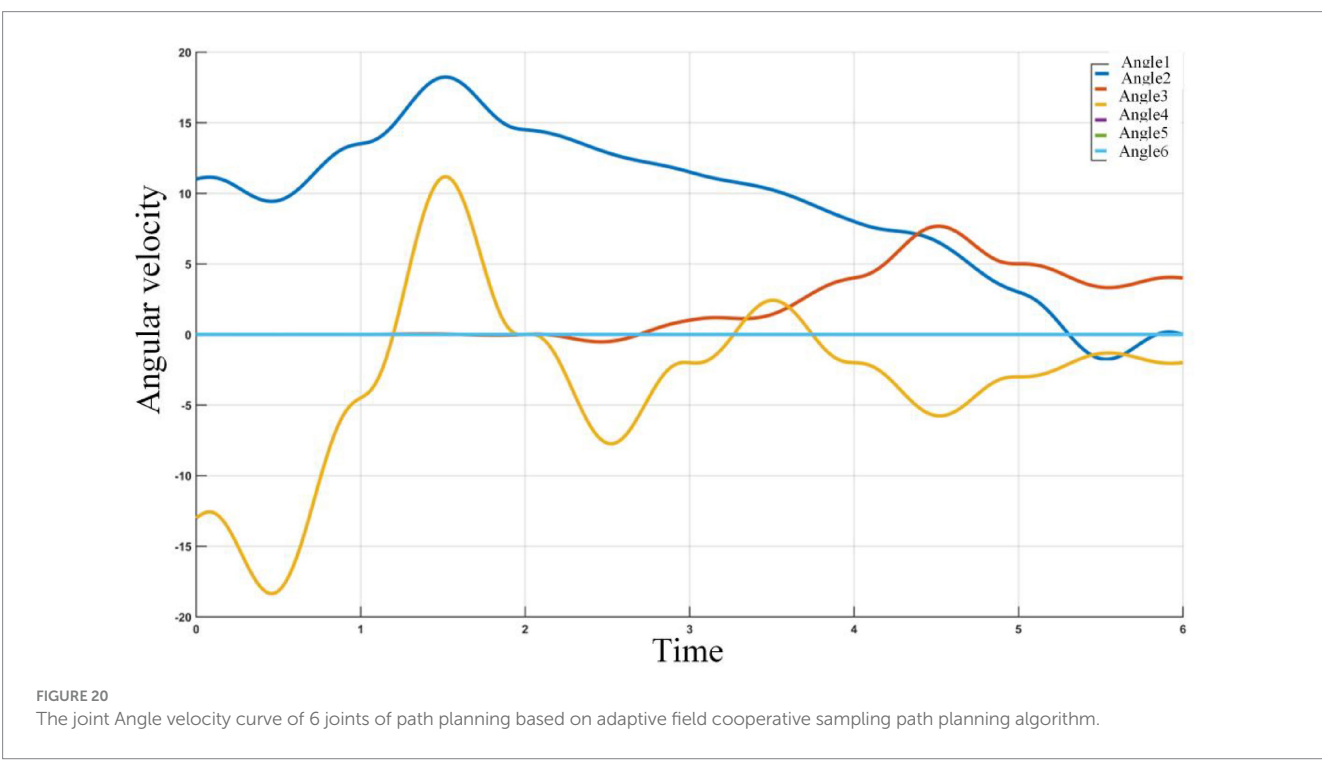
Category of parameters	Parameters		
Intrinsic parameter of left camera	$f_X$ =21.853, $f_Y$ =20.206, $c_X$ =22.023, $c_Y$ =612.37		
Radial distortion parameters of the left camera	$k_1 = -0.0108, k_2 = 0.3905, k_3$ = -0.9366		
Tangential distortion parameters of the left camera	p <sub>1</sub> = - 0.0257, p <sub>2</sub> = 0.0113		
Intrinsic parameter of right camera	$f_X$ =21.234, $f_Y$ =21.379, $c_X$ =21.666, $c_Y$ =609.82		
Radial distortion parameters of the left camera	k <sub>1</sub> = 0.0149, k <sub>2</sub> = 0.0693, k <sub>3</sub> = - 0.1083		
Tangential distortion parameters of the right camera	ρ <sub>1</sub> = - 0.0210, ρ <sub>2</sub> = 0.0135		
External parameters of binocular camera	R=[0.9906 0.0053 0.0121 -0.0055 0.9889 0.0002 -0.0131 -0.0103 0.9809] T=[-191.2268-6.7915 -31.7064]		

path planning algorithm can drive industrial robots to obtain a collision-free smooth path. The process of path planning of industrial robots based on adaptive field cooperative sampling algorithm is shown in Figure 21.

### 4 Conclusion

This article studies the path planning of industrial robots from the unique perspective of improving the intelligence of path planning algorithm. And an AFCS algorithm with strong environmental adaptability is proposed. It uses the traditional RRT algorithm as the





main framework to realize path planning. For the disadvantages of redundant sampling and low efficiency of the traditional RRT algorithm, this paper designs an optimal sampling strategy and improves the node expansion stage. The optimal sampling strategy not only solves the problem of redundant sampling, but also improves the quality of sampling points. The optimal sampling strategy is also beneficial to improve the path optimality. In the expansion stage, this

paper firstly improves the traditional APF algorithm, and then introduces it to the node expansion stage of the traditional RRT algorithm. This approach provides a theoretical basis for the generation of new nodes and improves the overall efficiency of the algorithm. More importantly, compared with other algorithms, the efficiency and practicability of the AFCS algorithm are improved, and the adaptability to the environment is significantly improved in the







Start point

Avoiding obstacles 1

Avoiding obstacles 2







Avoiding obstacles 3

Avoiding obstacles 4

Grasp the target

FIGURE 21

The process of path planning of industrial robots based on adaptive field cooperative sampling algorithm.

path planning of industrial robots. This approach not only provides ideas for the intelligent development of path planning algorithms, but also provides guarantees for the intelligent development of industrial robots.

### Data availability statement

The raw data supporting the conclusions of this article will be made available by the authors, without undue reservation.

### **Author contributions**

YZ: Investigation, Writing – original draft. SL: Formal analysis, Methodology, Writing – review & editing. QL: Investigation, Writing – original draft. DC: Conceptualization, Project administration, Writing – review & editing. WB: Formal analysis, Supervision, Writing – review & editing. XL: Investigation, Resources, Writing – review & editing. MF: Supervision, Visualization, Writing – original draft. LW: Investigation, Resources, Writing – original draft.

### **Funding**

The author(s) declare that financial support was received for the research and/or publication of this article. This work is supported by the Taishan Scholar Project of Shandong Province (tshw201502042), National Natural Science Foundation of China (NO.52206096).

### Conflict of interest

 $\operatorname{MF},\operatorname{XL}$  were employed by Datang Shandong Power Generation Co., Ltd.

The remaining authors declare that the research was conducted in the absence of any commercial or financial relationships that could be construed as a potential conflict of interest.

### Generative AI statement

The authors declare that no Gen AI was used in the creation of this manuscript.

Any alternative text (alt text) provided alongside figures in this article has been generated by Frontiers with the support of artificial intelligence and reasonable efforts have been made to ensure accuracy, including review by the authors wherever possible. If you identify any issues, please contact us.

### Publisher's note

All claims expressed in this article are solely those of the authors and do not necessarily represent those of their affiliated organizations, or those of the publisher, the editors and the reviewers. Any product that may be evaluated in this article, or claim that may be made by its manufacturer, is not guaranteed or endorsed by the publisher.

### References

Ahmadi, B., Zakeri, E., and Xie, W.-F. (2022). Optimal image-based task-sequence/path planning and robust hybrid vision/force control of industrial robots. *IEEE Access* 10, 26347–26368. doi: 10.1109/ACCESS.2022.3156919

Biao, H., and Cao, Z. (2021). Meng Chu Zhou, an efficient RRT-based framework for planning short and smooth wheeled robot motion under inodynamic constraints. *IEEE Trans. Ind. Electron.* 68, 3292–3302. doi: 10.1109/TIE.2020.2978701

Chi, W., Ding, Z., Wang, J., Chen, G., and Sun, L. (2022). A generalized Voronoi diagram-based efficient heuristic path planning method for RRTs in Mobile robots. *IEEE Trans. Ind. Electron.* 69, 4926–4937. doi: 10.1109/TIE.2021.3078390

Fan, X., Guo, Y., Liu, H., Wei, B., and Lyu, W. (2020). Improved artificial potential field method applied for AUV path planning. *Math. Probl. Eng.* 2020, 1–21.

Gammell, Jonathan D., Srinivasa, Siddhartha S., and Barfoot, Timothy D., Informed RRT\*: optimal sampling-based path planning focused via direct sampling of an admissible ellipsoidal heuristic. The IEEE RSJ international conference on intelligent robots and sys-tems (IROS) (2014).

Ganesan, Sivasankar, and Natarajan, Senthil Kumar, Asokan Thondiyath, G-RRT\*: Goal-oriented sampling-based RRT\* path planning algorithm for mobile robot navigation with improved convergence rate. Advances in robotics -5th international conference of the robotics society (2021) 1-6.

Guan-Zheng, T. A. N., and Huan, H. E. (2007). Aaron SLOMAN, Ant Colony System Algorithm for Real-Time Globally Optimal Path Planning of Mobile Robots. *Acta Automatica Sinica* 33, 279–285.

Guo, T., Wang, J., Wang, Z., Chen, W., Chen, G., and Zhang, S. (2022). Research on path planning of Mobile robot with a novel improved artificial potential field algorithm. *Math. Probl. Eng.* 2022, 1–13. doi: 10.1155/2022/5692350

Hart, P. E., Nilsson, N. J., and Raphael, B. (1972). A formal basis for the heuristic determination of minimum cost paths. *IEEE Trans. Syst. Sci. Cybernetics* 4, 28–29.

Hartenberg, R., Danavit, J., and Freudenstein, F. (1964). Kinematic synthesis of linkages. New York: McGraw-Hill.

Hong, B., Lin, Z., Chen, X., Hou, J., Lv, S., and Gao, Z. (2022). Development and application of key technologies for guide dog robot: a systematic literature review. *Robot. Auton. Syst.* 154:104104. doi: 10.1016/j.robot.2022.104104

Jia, L., Huang, Y., Chen, T., Guo, Y., Yin, Y., and Chen, J. (2022). MDA + RRT: a general approach for resolving the problem of angle constraint for hyper-redundant manipulator. *Expert Syst. Appl.* 193:116379. doi: 10.1016/j.eswa.2021.116379

Junxiang, X., and Wang, J. (2021). Effective motion planning of manipulator based on SDPS-RRTConnect. *Robotica* 40, 1855–1867. doi: 10.1017/80263574721001417

Kabutan, R., and Nishida, T. (2018). Motion planning by T-RRT with potential function for vertical articulated robots. *Electric. Eng. Japan* 204, 34–43. doi: 10.1002/eej.23103

Kang, G. (2019). Yong bum Kim, young Hun Lee, Hyun Seok Oh, won Suk You, Hyouk Ryeol Choi, sampling-based motion planning of manipulator with goal-oriented sampling. *Intell. Serv. Robot.* 12, 265–273. doi: 10.1007/s11370-019-00281-y

Kang, Gitae, Kim, Yong Bum, You, Won Suk, Lee, Young Hun, Oh, Hyun Seok, Moon, Hyungpil, et al., Sampling-based path planning with goal oriented sampling. 2016 IEEE international conference on advanced intelligent mechatronics (AIM) (2016) 1285.

Karman, S., and Frazzoli, E. (2011). Sampling-based algorithms for optimal motion planning. Int. J. Robotics Res. 30,846-894. doi: 10.1177/0278364911406761

Kavraki, L. E., Svestka, P., Latombe, J.-C., and Overmars, M. H. (1994). Probabilistic roadmaps for path planning in high-dimensional configuration spaces. *IEEE Trans. Robot. Autom.* 12, 566–580.

Khan, A. T. (2020). Shuai Li, Seifedine Kadry, Yunyoung Nam, control framework for trajectory planning of soft manipulator using optimized RRT algorithm. *IEEE Access* 8, 171730–171743. doi: 10.1109/ACCESS.2020.3024630

Khatib, O. (1986). Real-time obstacle avoidance for manipulators and Mobile robots. *Int. J. Robotics Res.* 5, 90–98. doi: 10.1177/027836498600500106

Larsena, L. (2017). Jonghwa Kimb \*, Michael Kupkea, Alfons Schuster, automatic path planning of industrial robots comparing sampling-based and computational intelligence methods. *Procedia Manufacturing* 11, 241–248. doi: 10.1016/j.promfg.2017.07.237

Lavalle, S., Rapidly-exploring random trees: A new tool forpath planning. [J] Computer Science. (1998).

Liu, B., Feng, W., Li, T., Chunhe, H., and Zhang, J. (2020). A variable-step RRT\* path planning algorithm for quadrotors in below-canopy.  $\it IEEE\ Access\ 8$ , 62980–62989. doi: 10.1109/ACCESS.2020.2983177

Lixing Liu, X., Wang, X. Y., Liu, H., Li, J., and Wang, P. (2023). Path planning techniques for mobile robots: review and prospect. *Expert Syst. Appl.* 227:120254. doi: 10.1016/j.eswa.2023.120254

Rostami, S. M. H. (2019). Arun Kumar Sangaiah, Xiaozhu Liu, Jin Wang, obstacle avoidance of mobile robots using modified artificial potential field algorithm. *EURASIP J. Wirel. Commun. Netw.* 2019, 1687–1690. doi: 10.1186/s13638-019-1396-2

Urain, J., Li, A., Liu, P., D'Eramo, C., and Peters, J. (2023). Composable energy policies for reactive motion generation and reinforcement learning. *Int. J. Robo. Res.*, 42, 1–14. doi: 10.1177/02783649231179499

Wang, J., Meng, M. Q. H., and Khatib, O. (2020). EB-RRT: optimal motion planning for Mobile robots. *IEEE Trans. Autom. Sci. Eng.* 17, 2063–2073. doi: 10.1109/TASE.2020.2987397

Wang, Ping, Xie, Xudong, Zheng, Hongxing, and Yu, Xiaoqiang, Rapid obstacle avoidance planning of patrol under multi-obstacle constraint [D], proceedings of 2021 international conference on autonomous unmanned systems (ICAUS 2021) (2022), pp. 3380–3387

Wang, D., Zheng, S., Ren, Y., and Danjie, D. (2022). Path planning based on the improved RRT\* algorithm for the mining truck. *Comp. Materials Continua* 71, 3571-3587. doi: 10.32604/cmc.2022.022183

Wei, K., and Ren, B. (2018). A method on dynamic path planning for robotic manipulator autonomous obstacle avoidance based on an improved RRT algorithm. *Sensors (Basel)* 18, 1424–1438. doi: 10.3390/s18020571

Yin, Q., Xiong, Z., and Zhang, G. (2018). Path planning for EOD robots. Int. J. Wireless and Mobile Computing 15, 223–229. doi: 10.1504/IJWMC.2018.096005

Yuan, Q., Yi, J., Sun, R., and Bai, H. (2021). Path planning of a mechanical arm based on an improved artificial potential field and a rapid expansion random tree hybrid algorithm. *Algorithms* 14, 813–819. doi: 10.3390/a14110321

Zhang, Z., Defeng, W., Jiadong, G., and Li, F. (2019). A path-planning strategy for unmanned surface vehicles based on an adaptive hybrid dynamic Stepsize and target attractive force-RRT algorithm. J Mar Sci Eng 7, 1–14. doi: 10.3390/jmse7050132